Molecular Biology of the Cell
Vol. 7, 1123–1136, July 1996

Structure–Function Studies of the Myosin Motor Domain: Importance of the 50-kDa Cleft

Kathleen M. Ruppel* and James A. Spudich†

Departments of Biochemistry and Developmental Biology, Stanford University School of Medicine, Stanford, California 94305

Submitted January 25, 1996; Accepted April 23, 1996
Monitoring Editor: J. Richard McIntosh

We used random mutagenesis to create 21 point mutations in a highly conserved region of the motor domain of *Dictyostelium* myosin and classified them into three distinct groups based on the ability to complement myosin null cell phenotypes: wild type, intermediate, and null. Biochemical analysis of the mutated myosins also revealed three classes of mutants that correlated well with the phenotypic classification. The mutated myosins that were not fully functional showed defects ranging from ATP nonhydrolyzers to myosins whose enzymatic and mechanical properties are uncoupled. Placement of the mutations onto the three-dimensional structure of myosin showed that the mutated region lay along the cleft that separates the active site from the actin-binding domain and that has been shown to move in response to changes at the active site. These results demonstrate that this region of myosin plays a key role in transduction of chemical energy to mechanical displacement.

INTRODUCTION

Cells undergo a wide variety of motile processes that are driven by molecular motors—enzymes that transduce the chemical energy of ATP hydrolysis into mechanical force and displacement. Three distinct groups of motors have been identified in eukaryotic cells: the actin-based myosin motors, the microtubule-based kinesin motor family, and dynein motor family. The last decade has witnessed an explosion in the identification of these proteins, and it is estimated that >50 molecular motors may be driving motile processes in a given cell. However, despite the ubiquity and utility of these enzymes, the molecular mechanism by which motor proteins convert chemical to mechanical energy is not fully understood.

The most extensively studied of the motor proteins is the myosin that drives muscle contraction, known as conventional myosin or myosin II. This protein has also been demonstrated in virtually all eukaryotic nonmuscle cells in which it is essential for processes such as cytokinesis (for review, see Spudich, 1989). It is known that the amino-terminal globular-head portion of myosin, termed subfragment 1 or S1, contains the catalytic and actin-binding properties of the molecule and is a functional motor unit in vitro (Toyoshima *et al.*, 1987; Kishino and Yanagida, 1988). Extensive kinetic analysis of the interaction of S1 with actin has led to a detailed description of the acto–S1 ATPase cycle. A simplified version of the model proposed by Lymn and Taylor (1971) to correlate this kinetic information with possible mechanical intermediates is summarized as follows: In the absence of ATP, actin and S1 form a tight or "rigor" complex. Binding of ATP to S1 greatly diminishes its affinity for actin, and the rigor complex is dissociated. ATP is then hydrolyzed to ADP and Pi by S1, and the hydrolysis products remain tightly bound. Actin interaction with the S1–ADP–Pi complex stimulates Pi release, which restores the high affinity of S1 for actin, resulting in formation of the tight actin–S1–ADP complex (strongly bound state). Subsequent ADP release returns the cycle to the rigor complex.

Attempts to understand the chemomechanical transduction mechanism of this system have been hampered by the lack of demonstrable mechanical/structural correlates for the states delineated in the enzymatic cycle. Recently, the high-resolution atomic structure of S1 from chicken skeletal muscle myosin

* Present address: Department of Medicine, Children's Hospital, 300 Longwood Avenue, Boston, MA 02115.
† Corresponding author.

(Rayment *et al.*, 1993b) and the docking of this structure, along with the actin structure of Kabsch *et al.* (1990) and Holmes *et al.* (1990) to electron micrographs of the rigor complex (Rayment *et al.*, 1993a; Schroeder *et al.*, 1993), has provided needed structural information and offered insights into the nature of the actin–myosin interaction.

Structural analysis reveals S1 to be highly asymmetric, consisting of a globular catalytic domain that contains the actin- and ATP-binding sites and a neck domain made of the carboxy-terminal portion of the heavy chain and two calmodulin-like light chains (Figure 1, top stereo pair). Within the catalytic domain, the actin- and ATP-binding sites are on opposite sides of the molecule (Rayment *et al.*, 1993a,b). These sites had previously been shown to be remote from each other (Botts *et al.*, 1989; Sutoh *et al.*, 1989). Because the kinetic data indicate that the binding affinity of S1 for actin changes upon binding of ATP and that product release from the active site is activated by binding of actin to S1, a question central to the understanding of chemomechanical transduction concerns the communication of these spatially distinct regions. Rayment *et al.* (1993a) hypothesized that this communication may be effected through changes in the narrow cleft that subdivides the central 50-kDa domain of the myosin head into upper and lower portions (the so-called 50-kDa cleft) (Figure 1, top). (The S1 head has been organized traditionally into three subdomains based on proteolytic studies that have revealed an NH_2-terminal 25-kDa region, a central 50-kDa segment, and a 20-kDa COOH-terminal segment.) This hypothesis is based on the following observations. The structure as solved has neither nucleotide nor actin bound to it and therefore may be captured in a structural state that is intermediate between these two configurations. The docking of the S1 and actin structures suggested that a better fit to the electron microscope (EM) image reconstructions would be obtained if this cleft were closed in the actin-bound state. Furthermore, potential actin–S1 interface contact sites are located on both sides of this cleft. In addition, analysis of the active site suggests that the binding site for the γ-phosphate would be located near or at the apex of the 50-kDa cleft (Rayment *et al.*, 1993b). Hence, it is possible that changes at one site may be transmitted through this central cleft to the other site and vice versa, providing a pathway for the transduction of this information. More support for the central role of this cleft comes from the recent solution of the crystal structures of the *Dictyostelium* motor domain in the presence of either beryllium or aluminum metallofluoride magnesium–ADP complexes (Fisher *et al.*, 1995). The beryllium fluoride complex is thought to mimic the ATP-bound/prehydrolysis state, whereas the aluminum fluoride complex seems to be closer to the ADP–Pi or posthydrolysis state. The structure of the complex with beryllium fluoride is essentially identical to the chicken structure, whereas the complex with aluminum fluoride exhibits significant domain movements, most notably of the lower portion of the 50-kDa domain that forms the lower border of this cleft. This suggests that hydrolysis of ATP induces a change in the cleft that may be transmitted to the actin-binding site and possibly the neck region of the molecule, as well.

Analysis of this cleft reveals that there is a high proportion of evolutionarily conserved residues making up its upper and lower borders, again supporting the idea that this region is pivotal to myosin function. Even before the structure of S1 was solved and available, we embarked on mutagenesis of this region simply on the basis of its strikingly high level of conservation. This region is too large to be amenable to classical site-directed mutagenesis techniques, because the number of potential changes is large and the usefulness of any given change is unknown. We therefore used a "directed random mutagenesis" approach and coupled it with an efficient in vivo screen to roughly ascertain the effects of the myosin mutations on motor function. This type of approach is possible with the cellular slime mold *Dictyostelium discoideum*, a highly motile eukaryote that has recently emerged as a leading organism for the in vivo and in vitro dissection of myosin function. Loss of myosin function in this organism leads to several well-characterized phenotypic defects (De Lozanne and Spudich, 1987; Knecht and Loomis, 1987; Manstein *et al.*, 1989), and the ability of a mutated myosin to complement these defects allows a quick in vivo screen of the functionality of a given mutant protein (Egelhoff *et al.*, 1991, 1993; Kubalek *et al.*, 1992; Uyeda and Spudich, 1993; Ruppel *et al.*, 1994; Uyeda *et al.*, 1994). The mutant enzyme can then be purified in milligram quantities and analyzed in vitro. The ability to screen mutant functionality in vivo makes possible a larger scale mutagenesis approach than would be otherwise feasible. Here we report the in vivo and in vitro characterization of a bank of random point mutations in this highly conserved region of the myosin head and discuss the biochemical defects caused by these changes in the context of the placement of these residues along the central cleft of the myosin motor domain.

MATERIALS AND METHODS

Plasmid Construction and Mutagenesis

Standard methods were used for all DNA manipulations (Sambrook *et al.*, 1989). A template for mutagenesis was created by first engineering into the *Dictyostelium mhc*A gene unique restriction sites that flanked the region to be mutagenized. Briefly, the unique *Xba*I site in the polylinker of pMyDAP (Egelhoff *et al.*, 1990) was destroyed by restricting with *Xba*I, blunting by treatment with Klenow fragment, and then religating. The plasmid was then restricted with *Pst*I and *Bgl*II, and the resultant 2.1-kilobase (kb) fragment was ligated into M13mp18 (Yanisch-Perron *et al.*, 1985) that had been

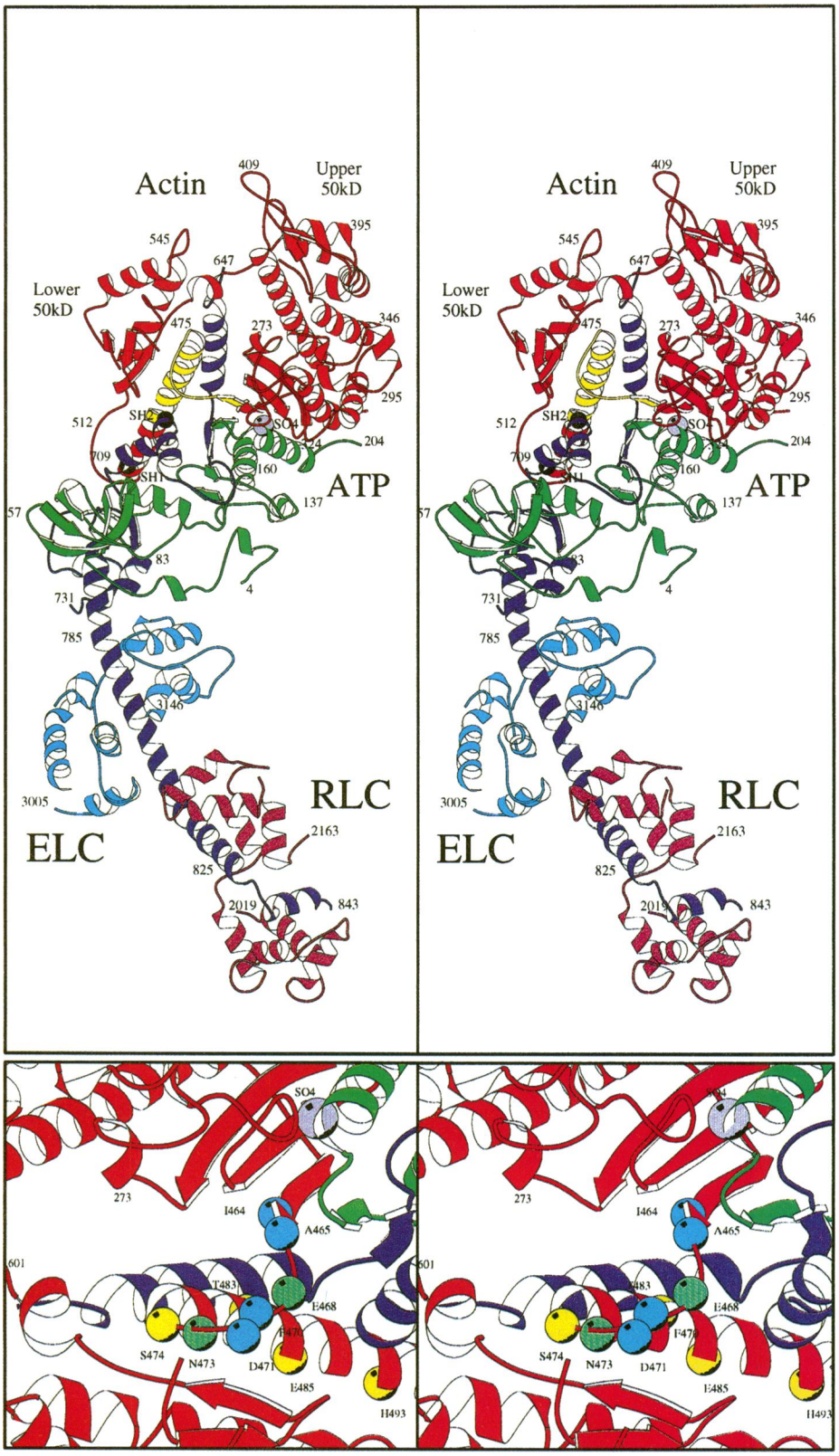

Figure 1. Stereo ribbon representation of the chicken skeletal muscle S1 structure showing the positions of the mutated residues. (A) The chicken S1 structure solved by Rayment *et al.* (1993b). The green, red, and blue segments represent the 25-, 50-, and 20-kDa segments of the heavy chain, and the cyan and magenta segments correspond to the essential and regulatory light chains, respectively. The ATP-binding site is noted, and a light purple ball has been added to the structure to approximate the location of the sulfate ion that in the chicken structure is found at the binding site for the β-phosphate of ATP. The yellow segment of the heavy chain indicates the region of the molecule mutagenized in this study. Note that this region begins at the apex of the long 50-kDa cleft just below and to the left of the ATP-binding site and then forms part of the lower border of the cleft. Orientation and labeling shown here are similar to views published by Reedy (1993) and are rotated ~140° from originally published views (Rayment *et al.*, 1993b). The actin-binding face, as defined by modeling of the chicken S1 and actin (Holmes *et al.*, 1990; Kabsch *et al.*, 1990) structures within the density of the acto–S1 complex as viewed by electron microscopy, is also depicted. Residue labels are indicated (2000 and 3000 have been added to the residue numbers of the regulatory and essential light chains, respectively). (B) This view of the chicken S1 structure is rotated ~90 degrees counterclockwise from that shown in A and focuses on the region of the head shown in yellow in part A. The color scheme is similar to part A, except that the mutated region is no longer highlighted in yellow. The individual residues mutated in the study are denoted by colored cpk representations of the appropriate α-carbon positions. The labels reflect the residue numbers for chicken skeletal muscle myosin (see alignment to *Dictyostelium* myosin shown in Figure 3). Several of the mutations leading to a wild-type phenotype [I464 (chicken) = I455V (*Dictyostelium*); A465 = S456L; F470 = F461Y; D471 = K462N—cyan cpk balls], intermediate phenotype [S474 = S465V; T483 = T474P; E485 = E476Q (also E476K in null class); H493 = H484Q—yellow cpk balls], or a null phenotype (E468 = E459V; N473 = N464K—light green cpk balls) are denoted. All ribbon diagrams were prepared with the program MOLSCRIPT (Kraulis, 1991).

restricted with *Pst*I and *Bam*HI to create M13MHC#4. Single-stranded uracil containing DNA was created by transforming M13MHC#4 into the *Escherichia coli dut⁻ ung⁻* strain CJ236 (Kunkel *et al.*, 1987). Site-directed mutagenesis was performed as described (Kunkel *et al.*, 1987) to simultaneously introduce a unique *Xho*I site at nucleotide 1247 and a unique *Xba*I site at nucleotide 1520. The sequences of the oligodeoxynucleotides used to create the mutations were *Xho*I: 5′-CGTTGAAAAATCCTCATCCTCGAGAGACGCTC-TTG-3′; and *Xba*I: 5′-CATCGATTTTGGTCTAGATTCACAAGCC-3′ (introduced restriction sites are underlined; introduced nucleotide changes are bolded). Neither mutation altered the amino acid sequence of the protein. Mutations were confirmed by dideoxy-sequencing. An M13MHC#4 isolate containing the introduced *Xho*I and *Xba*I sites was digested with *Bam*HI and *Bst*XI, and the resultant 2.0-kb fragment was cloned into pBIGMyD (Ruppel *et al.*, 1994), which had been restricted with *Bam*HI and *Bst*XI, thus replacing the 5′ portion of the wild-type *mhc*A gene with a version containing the unique *Xho*I and *Xba*I sites, creating pBIGMyD-X/X.

The 273 nucleotide *Xho*I-*Xba*I fragment of the *mhc*A gene was then subcloned into pBluescript II SK (Stratagene, La Jolla, CA), re-excised as a *Kpn*I-*Xba*I fragment, and subcloned into both M13mp18 and M13mp19, which had been digested with *Kpn*I and *Xba*I, to create M13MHC#7 and M13MHC#8, respectively. These vectors were used as templates for mutagenesis of the 50-kDa area of the *mhc*A gene. Single-stranded uracil containing DNA of each template was made, and site-directed mutagenesis was performed as above. The oligo HA is a 68mer that corresponds to the *mhc*A sequence 1336–1404 and was used to prime synthesis from the M13MHC#7 template. The oligo AN is a 66mer that corresponds to the *mhc*A sequence from nucleotide 1387–1453 and was used to prime synthesis from the M13MHC#8 template. Both oligos were synthesized with nucleotide precursors that were 97% of the appropriate precursor and 1% each of the other three nucleotide precursors to create a pool of slightly degenerate oligos that, on average, contained 1.5 nucleotide changes per oligo. Individual transformants resulting from the HA and AN synthesis reactions were screened for mutations by dideoxy-sequencing. Individual mutants were subcloned as *Xho*I-*Xba*I fragments into pBIGMyD-X/X that had been restricted with *Xho*I and *Xba*I.

Manipulation of Dictyostelium Cells

Dictyostelium cells were grown in HL5 medium, and development on 2-(*N*-morpholino)ethanesulfonic acid (MES) agar plates and bacterial lawns was performed as described previously (Ruppel *et al.*, 1994).

Transformations were performed essentially as described previously (Egelhoff *et al.*, 1991). The *mhc*A null cell line HS1 (Ruppel *et al.*, 1994) was transformed with 10 μg of each of the pBIGMyD-X/X plasmids bearing the different point mutations or a wild-type control, pBIGMyD. Cell lines that were able to grow in HL-5 supplemented with penicillin, streptomycin, and 8.5 μg/ml G-418 were isolated and subjected to further analysis.

Electrophoretic Methods

SDS-polyacrylamide gel electrophoresis and Western blot analysis of protein samples were performed with standard conditions as described previously (Ruppel *et al.*, 1994). Whole-cell lysates of *Dictyostelium* cells were prepared as described previously (De Lozanne and Spudich, 1987). Filters were probed with the monoclonal anti-*Dictyostelium* myosin antibody My6 (Peltz *et al.*, 1985) and developed with a horse-radish peroxidase-coupled secondary antibody (Bio-Rad Laboratories, Richmond, CA) and an enhanced chemiluminescence detection system (Amersham, Arlington Heights, IL).

Urea-SDS-glycerol polyacrylamide gel electrophoresis was performed by modification of the method of Perrie *et al.* (1973), as described by Ruppel *et al.* (1994).

Protein Purification

Purification of full-length wild-type and mutated myosins was performed with the method of Ruppel, Uyeda, and Spudich (Ruppel *et al.*, 1994). Briefly, this protocol consists of cell lysis in an EDTA-containing low-salt buffer, extraction of myosin from the insoluble fraction with a MgATP-containing high-salt buffer, and two rounds of salt-dependent assembly–disassembly of myosin filaments. The purified proteins were treated with *Dictyostelium* myosin light chain kinase, as described (Ruppel *et al.*, 1994).

Rabbit skeletal muscle actin and myosin were purified by the methods of Spudich and Watt (1971) and Margossian and Lowey (1982), respectively. The concentrations of these proteins were determined spectrophotometrically by using extinction coefficients of 0.62 cm^2/mg at 290 nm for actin (Spudich and Watt, 1971) and 0.53 cm^2/mg at 280 nm for myosin (Margossian and Lowey, 1982). Concentrations of the purified *Dictyostelium* myosins were determined by the method of Bradford (1976) with the use of rabbit skeletal muscle myosin as the standard.

Actin Cosedimentation Assays

Purified wild-type and mutant myosins at concentrations of 0.1 mg/ml were incubated with rabbit skeletal actin (0.2 mg/ml) in a buffer consisting of 10 mM HEPES pH 7.4, 200 mM KCl, 1 mM dithiothreitol (DTT), and 5 mM EDTA on ice for 15 min and then centrifugated at 75,000 rpm for 10 min in a Beckman TLA 100.1 rotor. The supernatant was removed and the pellet resuspended in 10 mM HEPES pH 7.4, 200 mM KCl, 4 mM $MgCl_2$, 2 mM ATP, and 1 mM DTT. The suspension was then clarified by centrifugation at 75,000 rpm for 10 min in a Beckman TLA100.1 rotor. Again the supernatant was removed and the pellet resuspended in SDS-gel sample buffer. Equal proportions of each supernatant and pellet fraction were then subjected to SDS-polyacrylamide gel electrophoresis.

ATPase Assays

The actin-activated ATPase activities of wild-type and mutated myosin were determined by measuring release of labeled Pi using [γ-32P]ATP by the protocol of Clarke and Spudich (1974), as modified by Ruppel (1994). Standard reaction mixtures for measuring actin-activated myosin ATPase activities contained 25 mM imidazole pH 7.4, 25 mM KCl, 4 mM $MgCl_2$, 1 mM DTT, 3 mM ATP, 0.1 mg/ml myosin, and 1 mg/ml actin. Reaction mixtures for determining low-salt MgATPase were as above, except that no actin was added. Reaction mixtures for high-salt Ca^{2+} and K^+-EDTA ATPase activities contained 0.6 M KCl, 25 mM imidazole pH 7.4, 3 mM ATP, 1 mM DTT, and either 5 mM $CaCl_2$ or 5 mM EDTA, respectively.

In Vitro Movement Assays

It has been shown that the presence of a small fraction of denatured myosin can be deleterious for in vitro movement assays (Warshaw *et al.*, 1990). Therefore, immediately before the motility assay, the solution of purified and phosphorylated myosin in 10 mM HEPES pH 7.4, 250 mM NaCl, 3 mM $MgCl_2$, 2 mM ATP, and 1 mM DTT was mixed with 0.1 mg/ml of filamentous rabbit skeletal muscle actin and sedimented at 55,000 rpm for 5 min in a Beckman TLA 100.1 rotor. This procedure removed denatured myosin that bound tightly to actin filaments in the presence of MgATP.

In vitro analysis of the movement of fluorescently labeled actin filaments over nitrocellulose surfaces coated with myosin was performed as described by Uyeda *et al.* (1990).

ATP Cross-linking Assays

Radiolabeled ATP was cross-linked to purified myosin by using a direct UV irradiation cross-linking protocol first adapted for use with myosin by Maruta and Korn (1981). Briefly, purified myosin at

0.5 mg/ml in a buffer containing 10 mM HEPES pH 7.4, 4 mM $MgCl_2$, and 1 mM DTT was incubated with either 20 μM [α-^{32}P]ATP or [γ-^{32}P]ATP on ice for 10 min and then irradiated at a distance of ~4 cm for 40 min with UV light at 254 nm on ice. Incorporation of ^{32}P was measured by spotting aliquots on Millipore (Bedford, MA) HAWP 02500 filters wetted with ice-cold 10% trichloroacetic acid (TCA), washing the filters under vacuum with 10 ml of ice-cold 10% TCA followed by 10 ml of ice-cold absolute ethanol, and counting the filters dissolved in 10 ml of Ready Safe scintillation fluid (Beckman Instruments, Fullerton, CA).

RESULTS

Mutagenesis and Expression of Wild-Type and Mutant mhcA Genes

To analyze the function of the highly conserved region of the 50-kDa domain of *Dictyostelium* myosin, we created a bank of random point mutations that blankets the region spanning residues 454–486 (corresponds to residues 463–495 of chicken muscle myosin). This was accomplished by synthesizing two slightly overlapping oligonucleotides corresponding to the region of interest for oligo-directed mutagenesis. The nucleotide precursors used to synthesize the oligos were contaminated with small, defined amounts of the other three nucleotide precursors such that the resultant pools of oligonucleotides contained mutations at random positions throughout the region of interest, and these pools of oligos were used to perform site-directed mutagenesis. Twenty-one independent mutant *mhc*A genes (excluding silent changes, stop codons, or deletions) were recovered from a screen of ~70 isolates. Of those 21 mutant genes, 15 contained single amino acid substitutions, 4 contained double amino acid substitutions, and the remaining 2 contained triple amino acid substitutions.

Each mutated *mhc*A gene was cloned into the expression plasmid pBIG, which contains a G418-resistant selectable marker and a *Dictyostelium* sequence that confers the ability to replicate extrachromosomally (Ruppel *et al.*, 1994). The resultant mutant *mhc*A expression plasmids were independently transformed into *Dictyostelium* cells lacking the endogenous *mhc*A gene (myosin null cells, HS1; Ruppel *et al.*, 1994). Clonal isolates expressing the appropriate mutated MHC polypeptide at levels comparable to the expression of MHC in the parental JH10 cell line were used for further analysis.

In Vivo Properties of Cells Expressing Mutated mhcA Genes

To quickly screen for the functionality of the altered myosins, HS1 cells expressing each mutant *mhc*A gene were assayed for their ability to undergo cytokinesis and form multicellular fruiting bodies upon starvation, processes that require functional myosin in *Dictyostelium*. This phenotypic analysis revealed three classes of mutants, which were termed wild type, null, or intermediate, based on their ability to develop (Figure 2) and grow in suspension (our unpublished observations).

Table 1 shows the classification of the point mutations by phenotype. In a random mutagenesis scheme, the effect of any given point mutation depends on two factors: the degree of amino acid sequence conservation at the mutated position and the nature of the amino acid change that is introduced. Therefore, for each of the 21 mutants, we analyzed both of these factors. The extent of sequence conservation for each residue was estimated by comparing the sequences of 32 myosin heavy chains by using a progressive (similarity) alignment (Sellers and Goodson, 1995). This group of myosins included 20 myosin II's from skeletal, smooth, and cardiac muscle as well as nonmuscle myosins and 12 myosin I's from a variety of subfamilies. Percentage conservation at a given position was calculated on the basis of the number of sequences that had the same residue as the *Dictyostelium* sequence at that position. The other residues found at that same position in the other myosins analyzed are also listed. Figure 3 shows a comparison of a subset of the analyzed sequences as well as the placement of each of the mutations, categorized by phenotypic class. The severity of the introduced change was estimated with the PAM250 scoring matrix, an amino acid replacement matrix developed by Dayhoff (1978).

The wild-type class of mutants fully complemented the ability of the myosin null cells to undergo normal fruiting body formation (Figure 2A) and grew in suspension culture with doubling times similar to that of the wild-type JH10 cell line or HS1 cells transformed with wild-type myosin. Seven single amino acid substitutions fell into this category (Figure 3 and Table 1), and each of these mutations was either a favorable (PAM250 > 1) substitution of a highly conserved residue (e.g., F461Y) or a less favorable substitution of a relatively nonconserved residue (e.g., S456L).

A second class of mutants behaved phenotypically as myosin null cells—members of this class were incapable of growth in suspension and arrested at the mound stage of *Dictyostelium* development (Figure 2C)—although they expressed myosin at levels comparable to wild-type controls (our unpublished observations). This category included three single amino acid substitutions that represent neutral to less favorable mutations of highly conserved residues (PAM250 ≤ 1), as well as all of the double and triple amino acid substitutions (Figure 3 and Table 1). This phenotypic class also included a mutated *mhc*A gene in which a 10-amino-acid portion of the 50-kDa region (amino acids 504–513) had been deleted (MHCΔ504–513).

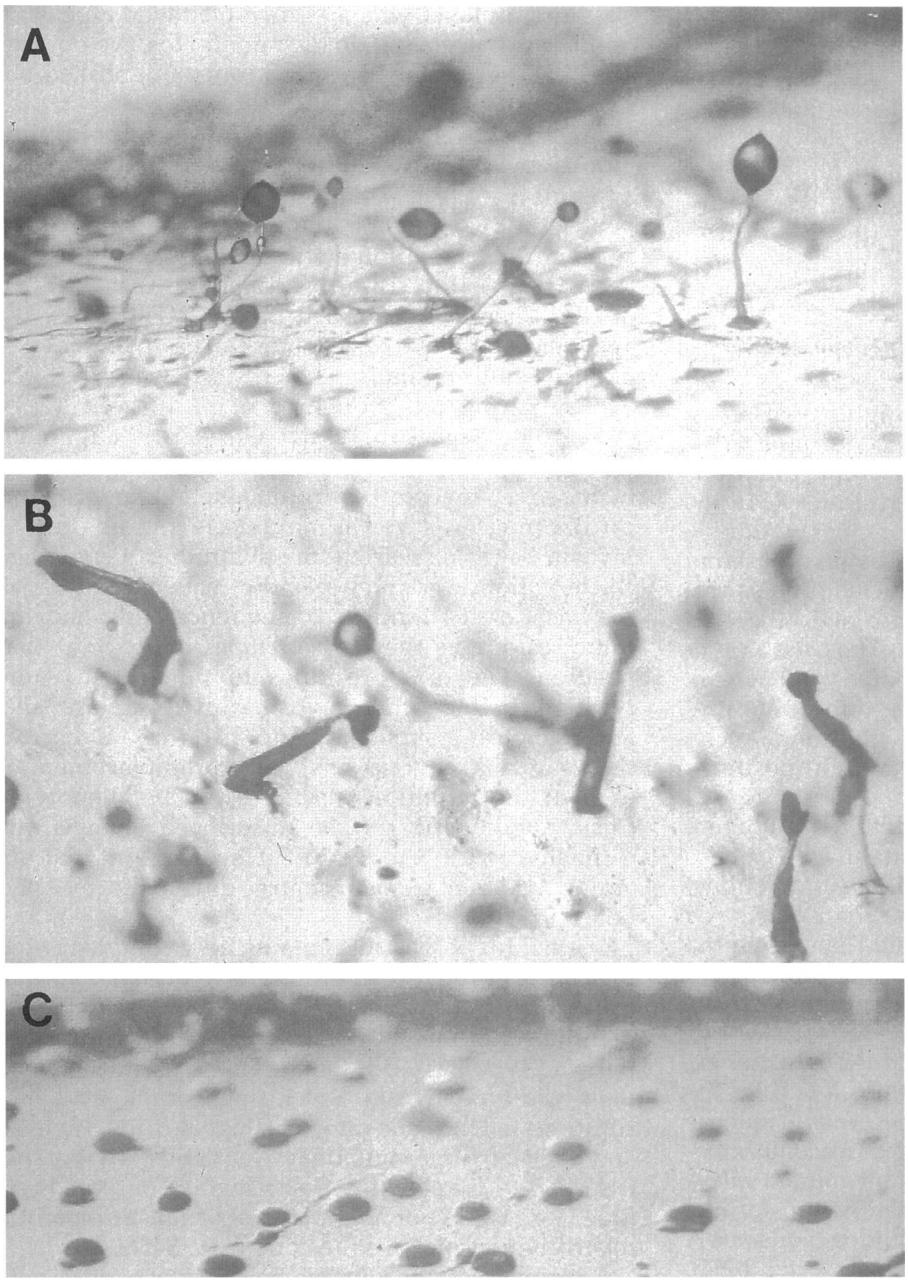

Figure 2. Development of *Dictyostelium* fruiting bodies. HS1 cells (*mhc*A$^-$) expressing myosin containing: (A) The F481V mutation as an example of the 'wild-type' phenotypic class, (B) the S465V mutation as an example of the 'intermediate' phenotypic class, or (C) the E459V mutation as an example of the 'null' phenotypic class. Mutants in the wild-type class formed fruiting bodies that were indistinguishable from those formed by the parent JH10 cell line, while mutants in the null class behaved as the myosin null line HS1 in that they arrested at the mound stage of *Dictyostelium* development. The mutants comprising the intermediate class were able to develop beyond the mound phase but rarely culminated in normal fruiting body formation.

A third class of mutants, termed intermediate, were capable of only partially complementing the myosin-specific defects of the HS1 cells. These mutants were capable of growth in suspension culture, although more slowly and to a lower density. Upon starvation they developed beyond the mound stage but rarely culminated in normal fruiting bodies (Figure 2*B*). Often they arrested as club-like stalks or slugs, and the fruiting bodies that did form were quite short; however, spores from these fruits were viable. This class was comprised of four single amino acid substitutions at relatively highly conserved positions (Figure 3 and Table 1).

In Vitro Analysis of Mutated Myosins

Cells expressing representative mutant myosins from each phenotypic class were grown, and the mutated myosins were individually purified from these cells with a protocol for purification of *Dictyostelium* myosin that depends largely on the filament-forming properties of the tail; thus this protocol should have been

Table 1. Classification of the myosin mutants

Mutation	Severity: PAM250 matrix score[a]	% Conservation at this position[b]	Other A.A. residues at this position[b,c]
I. Wild-type class			
I455V	4	94	M2
S456L	−1	6	A18, Y8, F4
F461Y	7	97	L1
K462N	1	3	E15, D12, Q2, G, N
Y473H	0	53	F14, T1
Y473S	−3	53	F14, T1
F481V	−1	50	L5, I4, E2, H2, Q, V, Y
II. Intermediate class			
S465V	−1	84	G5
T474P	0	53	V9, A3, C2, L
E476Q	2	100	
H484Q	3	59	Q6, E3, D, L, M, N
III. Null class			
E459V	−2	100	
N464K	1	100	
E476K	0	100	
E459A/I460N	0/−2	100/88	H2, C, T
N475I/E476Q	−2/2	100/100	
C470G/Q479P	−3/0	78/100	W4, I, M, V
F481C/N483K	−4/1	50/78	L5, I4, E2, H2, Q, V, Y/I7
N472M/N475K/L478I	−2/1/2	100/100/97	M1
Y473S/K477N/F481C	−3/1/−4	53/88/50	F14, T1/R2, Q, T/L5, I4, E2, H2, Q, V, Y
MHCΔ504-513	na	na	

Mutated myosins were grouped according to their ability to phenotypically complement the myosin specific defects of the myosin (*mhc*A) null cells upon transformation (see text for details). For each mutation, we have scored the severity of the amino acid change as well as the degree of conservation at the position of the mutated residue. One letter abbreviations are used to indicate the amino acid changes at the indicated positions.

[a] Based on the PAM250 scoring matrix, an amino acid replacement matrix developed by Dayhoff, 1978. See text for details.

[b] Based on progressive (similarity) alignment of 32 myosin heavy chain sequences (Sellers and Goodson, 1995). Included in the alignment were 20 myosin II's, and 12 myosin I's, including the *Drosophila nina*C myosin.

[c] Listed are the other amino acid residues present at that position in the 32 myosins included in the alignment, followed by the number of times represented.

less affected by changes to the motor domain of myosin (Ruppel *et al.*, 1994). Several mutants in each class were purified to homogeneity for subsequent analysis of kinetic and motile properties (representative purification gel shown in Figure 4A). Because these properties are affected by the extent of regulatory light chain phosphorylation of *Dictyostelium* myosin (Griffith *et al.*, 1987; Ruppel *et al.*, 1994), each myosin was then treated with *Dictyostelium* myosin light chain kinase, and the extent of regulatory light chain (RLC) phosphorylation was assayed by urea-SDS-glycerol PAGE (Ruppel *et al.*, 1994). (In every case, RLC phosphorylation was ≥90%; see Figure 4B.) This ensured that comparisons between mutants and between different preparations of the same mutant were meaningful. Routine analysis included assays for the ability to interact with actin in an ATP-dependent manner, solution ATPase activities—both low-salt MgATPase activity in the presence and absence of actin and high-salt ATPase activities—and our in vitro movement assay.

Three of the single amino acid substitution mutants from the wild-type class, Y473H, Y473S, and F481V, were purified and analyzed (Table 2). All three exhibited normal to slightly elevated low-salt MgATPase activities; the actin-activated ATPase activities were all ~30–50% of wild-type myosin values (Table 2). Velocities of actin filament translocation in an in vitro movement assay were also somewhat variable among myosins in this class, and all were slightly slower than wild-type myosin velocities (Table 2).

Three of the single amino acid substitution mutants from the intermediate class, S465V, T474P, and E476Q, were also purified and analyzed (Table 2). The biochemical properties of myosins from this class were somewhat more variable. The S465V myosin exhibited a high basal MgATPase activity (103 ± 22 nmol Pi/min/mg) relative to wild type (12 ± 4 nmol Pi/min/mg) and was activated approximately twofold by ac-

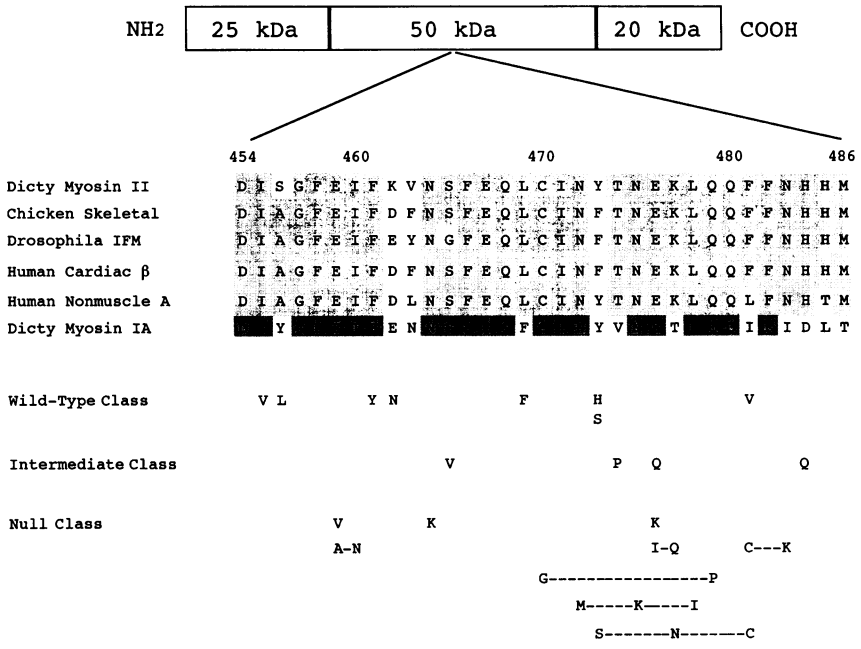

Figure 3. Comparison of amino acid sequences of various myosin heavy chains in the region of the highly conserved 50-kDa domain mutagenized in this study and placement of mutated residues on the alignment by phenotypic class. Included in the alignment are myosin II's from *Dictyostelium discoideum* (PIR A26655); chicken skeletal muscle (Swiss-Prot P13538); *Drosophila melanogaster* indirect flight muscle, including exon 9a (PIR A32491); human cardiac muscle (Swiss-Prot P12883) and human nonmuscle (PIR M81105); and a myosin I from *Dictyostelium discoideum* (Swiss-Prot P22467). Amino acid residue numbers correspond to the *Dictyostelium* myosin II sequence (line 1). (This stretch corresponds to residues 463–495 of chicken myosin.) Residues appearing in four of the five myosin II sequences at any given position are shaded light gray to denote sequence conservation. Conservation at these positions in the myosin I sequence is denoted by dark gray shading (line 6). The amino acid substitutions that comprise the mutations analyzed in this study are shown in the bottom portion of the figure. The mutations fell into three phenotypic classes when transformed into HS1 (*mhc*A$^-$) cells (wild type, intermediate, and null; see text for details) and are grouped according to this classification. Each substitution is shown under the residue it replaces; double- and triple-residue changes in the same mutant are indicated by dashed lines connecting each individual change.

tin to give an actin-activated ATPase activity (226 ± 30 nmol Pi/min/mg) that was slightly higher than wild type (170 ± 20 nmol Pi/min/mg). However, this mutant myosin moved actin filaments at only 0.2 ± 0.1 μm/s, which was approximately one-tenth the speed of wild-type myosin (2.2 ± 0.2 μm/s). The quality of the movement was smooth, with little fragmentation of actin filaments, and the velocity was not affected by cycling the myosin through rounds of actin–affinity centrifugation to remove denatured myosin heads. This suggested that the slow movement was not due to denatured or rigor heads. Thus, this amino acid substitution differentially affected the solution ATPase and mechanical displacement properties of myosin, effectively uncoupling ATP hydrolysis from movement of actin filaments. One possible explanation for these results was that this mutation caused an increase in the affinity of the myosin for actin, which would increase the solution actin-activated ATPase activity but might decrease the velocity in vitro by increasing the affinity of myosin for actin either during the weakly or strongly bound state (see DISCUSSION for details). To test this possibility, motility assays were performed on surfaces that had been coated with 50–50 mixtures of wild-type and S465V myosins either as monomers or as mixed filaments. At saturating myosin surface densities, the mixed surfaces supported movement of actin filaments at rates (2.0 ± 0.3 μm/s) similar to those produced by wild-type myosin alone, suggesting that the S465V myosin was not exerting its effects through increased load on the actin filament.

The T474P and E476Q mutants also exhibited variable degrees of uncoupling of solution actin-activated ATPase activity from in vitro motility, although both myosins were significantly less active than the S465V myosin overall (Table 2). The T474P myosin had a normal low-salt MgATPase but displayed an actin-activated ATPase activity that was ~fivefold lower than wild-type myosin. The effect of the mutation on in vitro motility was much greater, however, as the T474P myosin moved actin filaments at a rate of 0.1 ± 0.04 μm/s, which is ~20-fold slower than wild type. The degree of uncoupling of these properties exhibited by the E476Q mutant was even greater. This mutated myosin had a normal basal activity and an actin-activated ATPase activity (51 ± 6 nmol Pi/min/mg) that was approximately threefold lower than wild-type activity, whereas its velocity in vitro was ~40-fold slower than wild type (0.1 ± 0.03 μm/s).

Several myosins from the null phenotypic class were purified for in vitro analysis, including three single amino acid substitutions, E459V, N464K, and E476K, and two double amino acid substitutions, N475I/E476Q and F481C/N483K. All of these mutated myosins behaved similarly in initial in vitro studies. There were no detectable low-salt MgATPase, actin-activated ATPase, high-salt Ca-ATPase, or high-salt K-EDTA ATPase activities for any of these proteins (Table 1). Furthermore, in the in vitro motility assay,

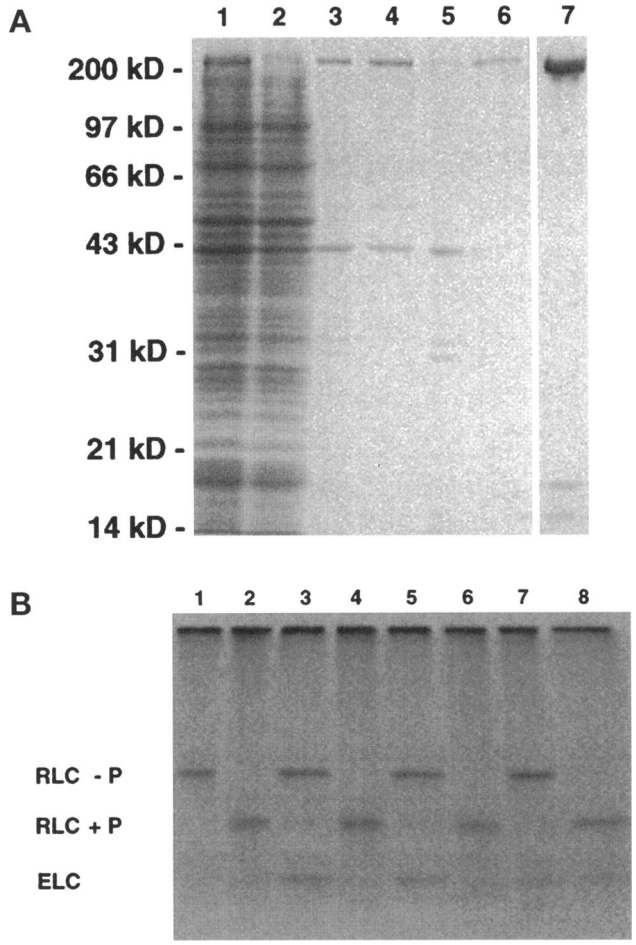

Figure 4. SDS-PAGE of fractions obtained during the purification of myosin from *Dictyostelium* and urea-SDS-PAGE analysis of regulatory light chain phosphorylation of purified myosins after treatment with myosin light chain kinase. (A) Coomassie Brilliant Blue-stained 12.5% gel of fractions obtained during the purification of the E459V myosin. Lane 1, Whole-cell lysate; lane 2, low-speed supernatant; lane 3, low-speed pellet; lane 4, ATP extraction high-speed supernatant; lane 5, ATP extraction high-speed pellet; lane 6, low-salt pellet; lane 7, purified E459V myosin. Molecular weight standards are noted at the left. (B) Coomassie Brilliant Blue-stained 7.5% urea-SDS-glycerol polyacrylamide gel of purified protein samples that were prepared for electrophoresis as described under MATERIALS AND METHODS is shown. Wild type (lanes 1 and 2), F481V (lanes 3 and 4), S465V (lanes 5 and 6), and E459V (lanes 7 and 8) were either untreated (lanes 1, 3, 5, and 7) or treated (8–12 h at 0°C; lanes 2, 4, 6, and 8) with *Dictyostelium* myosin light chain kinase. Twenty micrograms of protein were loaded in each lane. Migration of the essential light chain (ELC) and both forms of the regulatory light chain (RLC + P and RLC − P) are noted at the left.

although each myosin would bind fluorescent actin filaments in the absence of ATP, upon addition of ATP the actin detached from the myosin-coated surface, and no movement was observed.

The in vitro motility results suggested that these myosins were capable of binding to actin in an ATP-dependent manner, and this was confirmed by actin cosedimentation assays (Figure 5). Therefore, it seemed most likely that these mutants were defective in some later step of the ATP chemomechanical cycle. The two most likely possibilities were that these myosins were either unable to hydrolyze ATP once it was bound or that they could hydrolyze the bound ATP but were unable to release the product ADP and/or Pi. To distinguish between these possibilities, we looked at the ability of three of these mutants to be cross-linked to radiolabeled ATP by a UV cross-linking technique originally modified for use with myosin by Maruta and Korn (1981). It is known that this cross-linking occurs via the adenine moiety of the nucleotide. The E459V, N464K, and E476K myosins, as well as wild-type myosin, were subjected to direct UV irradiation in the presence of either α- or γ-^{32}P-ATP and then separated from the non-cross–linked label under denaturing conditions by TCA precipitation. In the case of wild-type myosin, appreciable cross-linked label was detected only in the sample incubated with the α-labeled ATP, whereas the mutant myosins retained the α- and γ-labeled ATP with similar efficiency (Figure 6). This suggests that the wild-type myosin was capable of hydrolyzing the bound nucleotide efficiently, resulting in the loss of the γ-label under denaturing conditions, whereas the mutants were unable to hydrolyze the bound nucleotide, resulting in equal retention of both the α- and γ-labels.

DISCUSSION

A major focus of research in the field of motor proteins concerns the molecular nature of the transduction of chemical energy into mechanical work. In the case of the actin-based motor myosin, this transduction event has been localized to the interaction between the globular head domain of myosin (S1) and the actin filament (Toyoshima *et al.*, 1987; Kishino and Yanagida, 1988). Models of muscle contraction have hypothesized that ATP-dependent movement and force production occur as a consequence of conformational changes within S1 while it is bound to the actin filament (Huxley, 1969; Huxley and Kress, 1985). A wealth of biochemical and biophysical data, coupled with recent advances in the structural analysis of actin and myosin, have provided new insights into the possible nature of these conformational changes. Based on docking studies of the crystal structures of actin and chicken S1, Rayment and coworkers (Rayment *et al.*, 1993a; Fisher *et al.*, 1995) have proposed a structural model for the actomyosin contractile cycle. Like many previous models, this modified version of the swinging cross-bridge model involves the amplification of conformational changes in the globular motor domain by the putative lever arm formed by the light chain-binding neck of S1. According to the model, swinging of the lever arm relative to the motor domain, which

Table 2. ATPase activities and sliding velocities of the myosin mutants

Mutation	Low-salt Mg^{2+}-ATPase activity (nmol Pi/min/mg)	Actin-activated ATPase activity (nmol Pi/min/mg)	High-salt Ca^{2+} ATPase activity (nmol Pi/min/mg)	High-salt K^{+}-EDTA ATPase activity (nmol Pi/min/mg)	Sliding velocity in vitro (μm/s)
WILD TYPE	12 ± 4	170 ± 20	655 ± 100	42 ± 12	2.2 ± 0.2
I. Wild-type class					
Y473H	15 ± 2	90 ± 15	655 ± 55	6	1.8 ± 0.2
Y473S	25 ± 3	50 ± 7	770 ± 40	2	1.7 ± 0.2
F481V	23 ± 4	65 ± 5	161 ± 24	5	1.2 ± 0.2
II. Intermediate class					
S465V	103 ± 22	226 ± 30	188 ± 22	11 ± 4	0.2 ± 0.1
T474P	8 ± 1	35 ± 5	6 ± 3	3	0.1 ± 0.04
E476Q	12 ± 3	51 ± 6	17 ± 2	2	0.1 ± 0.03
III. Null class					
E459V	n.d.	n.d.	n.d.	n.d.	f.d.
N464K	n.d.	n.d.	n.d.	n.d.	f.d.
E476K	n.d.	n.d.	n.d.	n.d.	f.d.
N475I/E476Q	n.d.	n.d.	n.d.	n.d.	f.d.
F481C/N483K	n.d.	n.d.	n.d.	n.d.	f.d.
MHCΔ504-513	n.d.	n.d.	n.d.	n.d.	f.d.

Mutated myosins are grouped according to their ability to phenotypically complement the myosin-specific defects of the myosin null cells upon transformation (see text for details). For each mutant, the solution ATPase activities and in vitro sliding velocities were determined as described in MATERIALS AND METHODS.

n.d.: None detected; f.d.: filaments detached.

remains strongly bound to actin at a fixed angle, results in displacement of the actin filament. Mutational, biochemical, and structural analysis of this lever arm region has lent support to this hypothesis (Itakura *et al.*, 1993; Lowey *et al.*, 1993; Uyeda and Spudich, 1993; Jontes *et al.*, 1995; Whittaker *et al.*, 1995; Spudich *et al.*, 1995; Uyeda *et al.*, 1996).

Central to this model are the conformational changes that occur within the globular portion of S1 in response to binding of actin and nucleotide and the coupling of these changes to "priming" of the putative lever arm. Structural studies have implicated the long narrow cleft that splits the central 50-kDa domain both in communication between the spatially distinct ATP- and actin-binding sites and in transmitting changes to the lever arm (Rayment *et al.*, 1993a,b; Fisher *et al.*, 1995). The apex of this cleft is located at the base of the nucleotide-binding pocket, and it extends out toward the actin-binding face of the molecule, where potential actin interaction surfaces are found on both sides of the cleft. The cleft is thought to be in the open conformation in the chicken S1 structure (Rayment *et al.*, 1993a,b) and in the *Dictyostelium* motor domain–beryllium fluoride complex (Fisher *et al.*, 1995), whereas in the ADP–aluminum fluoride-bound *Dictyostelium* structure, which is thought to mimic the transition state of ATP hydrolysis, this cleft is partially closed. Docking studies of the crystal structure suggest that the best fit of the chicken S1 structure to the rigor complex would involve complete closure of this cleft. Combining these observations, the following model has been proposed (Fisher *et al.*, 1995): In the rigor complex, the cleft is closed with actin bound. Binding of ATP with placement of the γ-phosphate at the apex of the cleft causes the cleft to open, resulting in dissociation of the rigor complex. Hydrolysis of ATP causes partial closure of the cleft, as defined by the changes seen in the *Dictyostelium* motor domain–ADP–aluminum fluoride complex. These changes are hypothe-

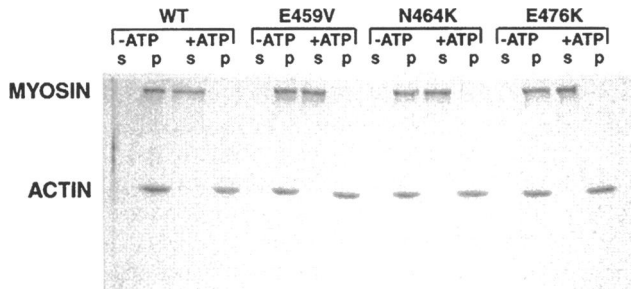

Figure 5. Cosedimentation of purified wild-type and mutant *Dictyostelium* myosins with actin in the presence and absence of ATP. Purified wild-type *Dictyostelium* myosin (WT), as well as three mutated myosins belonging to the null phenotypic class (E459V, N464K, and E476K; see text for details), was incubated with rabbit skeletal actin in the absence of ATP and then centrifugated as described in MATERIALS AND METHODS. The resultant pellet was resuspended in a MgATP-containing buffer and again centrifugated as described. Aliquots of supernatants (s) and pellets (p) from each centrifugation were then subjected to SDS-polyacrylamide gel electrophoresis.

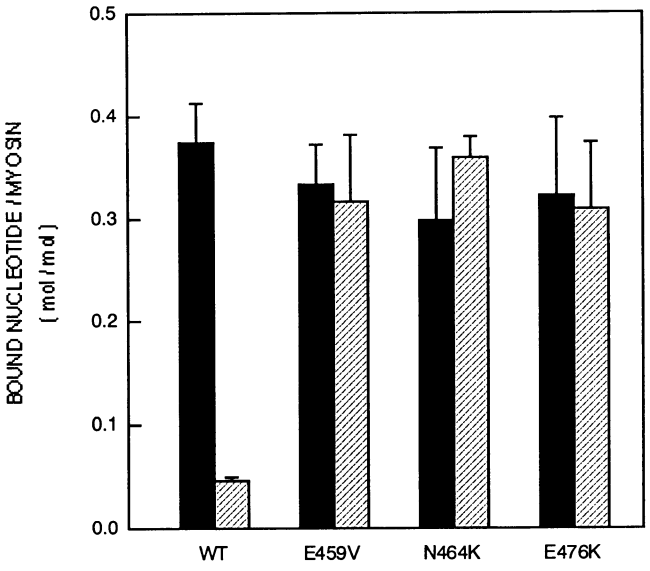

Figure 6. Photoaffinity labeling of purified wild-type and mutant *Dictyostelium* myosins with radioactive ATP. Purified wild-type *Dictyostelium* myosin, as well as three mutated myosins belonging to the null phenotypic class (see text for details), was mixed with either [α-^{32}P]ATP (solid black fill) or [γ-^{32}P]ATP (light hatched fill), irradiated with UV light, and then assayed for bound nucleotide as described under MATERIALS AND METHODS. Efficiency of photolabeling depended on the concentration of nucleotide and the length of time of UV irradiation. The efficiency of photolabeling of [α-^{32}P]ATP to wild-type and mutant myosins shown here is close to that reported for *Acanthamoeba* myosin II (0.38 mol/mol) under similar conditions (Maruta and Korn, 1981).

sized to cause conformational changes in the adjacent reactive thiol region that ultimately result in "priming" of the lever arm. Rebinding of actin in the tightly bound state induces complete closure of the cleft and displacement of Pi from the base of the nucleotide cleft. This cleft closure is proposed to cause further changes in the carboxy-terminal portion of the molecule, resulting in a conformational change in the lever arm that gives rise to the power stroke and returns the complex to the rigor state.

Analysis of this 50-kDa cleft reveals that it is lined with a high proportion of evolutionarily conserved residues. Before solution of crystal structures of the myosin motor domain, we targeted for mutagenesis regions of the head that exhibited high degrees of sequence conservation whose function was unknown, including a region of the central 50-kDa domain that turns out to form the apex and lower border of this important cleft (Figure 1). We have combined oligo-mediated random mutagenesis techniques with quick in vivo screens for myosin functionality to create and analyze a large bank of point mutations in this region. A group of 21 point mutations in the region spanning residues 454–486 of *Dictyostelium* myosin (corresponding to residues 463–495 of chicken skeletal muscle myosin) were recovered and transformed into myosin null cells. These mutated myosins were placed into three phenotypic classes (wild type, null, and intermediate) on the basis of their ability to complement the cytokinesis and developmental defects (Figure 3) of the myosin null cells. Representative mutants from each class were then purified and characterized in vitro. We found that the in vivo and in vitro properties of the mutated myosins correlated well. The wild-type–like class of myosins were able to fully complement the myosin-specific defects of the null cells and exhibited relatively normal solution ATPase activities and sliding velocities in vitro. (However, it is interesting to note that two of the three mutations tested in vitro displayed ATPase activities and sliding velocities that were approximately one-half that of the wild-type myosin. Nonetheless, these altered myosins fully complemented the defects of the null cells, suggesting that the in vivo assays used are not extremely sensitive to changes in myosin motor function.) Mutations that gave rise to myosins in this class tended to be either favorable substitutions of highly conserved amino acids or changes at relatively nonconserved positions (Table 1). One of the mutations that fell into this class changed the highly conserved isoleucine residue (Ile455Val, chicken residue I464 in Figure 1, bottom stereo pair) that is one of two residues around which main chain conformational angle changes occur.The changes result in the partial closure of the cleft seen in the *Dictyostelium* motor domain–ADP–aluminum fluoride structure. It is possible that the conservative isoleucine to valine change does not affect the ability of this loop to undergo this conformational change. However, as was discussed above, the wild-type phenotype in vivo does not preclude a minor defect in motor activity in vitro.

In contrast to the wild-type–like group, the null class contained myosins with unfavorable single-point mutations in highly conserved residues, as well as all the double- and triple-point mutations recovered in the screen. All of these proteins were expressed in the cells at levels comparable to wild type and were stable to purification; hence, the phenotypic defect was due to loss of motor function of the myosin and not due to loss of the myosin itself. Purification of several of these myosins revealed that they exhibited a defect in hydrolysis of ATP. These myosins bind actin in the absence of nucleotide and dissociate from actin upon addition of ATP; however, these myosins exhibited no detectable ATPase activity and were incapable of supporting movement of actin filaments in sliding filament assays. (The lower limit of reliable detectability for these assays is ~0.5–1.0 nmol Pi/min/mg, which represents a 200- to 400-fold drop from wild-type actin-activated ATPase activity and a 600- to 1200-fold drop in high-salt Ca-ATPase activity.) These observations suggested that these mutations caused

the myosins to arrest or at least severely slow down at a point in the actomyosin–ATPase cycle after binding of ATP but before release of products. (Solution ATPase assays quantitate release of free Pi.) The two most likely possibilities are either that they failed to hydrolyze ATP (or that the back reaction was greatly favored) or that they hydrolyzed ATP and were unable to release the products. ATP cross-linking studies confirmed that the defect was in hydrolysis (Figure 6). This defect before hydrolysis prevents high-affinity rebinding of actin in the prestroke state. Thus, these myosins are unable to interact productively with actin to produce force, resulting in no detectable ATPase activity, the inability to translocate actin filaments in vitro, and a myosin null phenotype in vivo. Kronert *et al.* (1994) discovered that a mutation in *Drosophila* indirect flight muscle that directly mimics the Glu476Lys change (position shown as chicken residue E485 in Figure 1, bottom) that led to this nonhydrolyzer defect/null phenotype in *Dictyostelium* myosin resulted in a null phenotype in *Drosophila* as well. Flies homozygous for this mutation failed to accumulate appreciable amounts of myosin or form thick filaments in the indirect flight muscle despite normal levels of mRNA. However, as would be expected from the nature of the biochemical defect of the *Dictyostelium* protein, this mutant myosin did not poison assembly of wild-type thick filaments in heterozygotes.

Placement of these mutations on the S1 structure (Figure 1, bottom) reveals that they are distributed throughout the mutagenized area of the lower cleft. Thus it seems unlikely that all of these residues play a direct role in ATP hydrolysis. However, it is possible that these mutations inhibit or alter conformational changes within the cleft that are necessary for hydrolysis to take place. In particular, the partial closure of the cleft seen in the *Dictyostelium*–ADP–aluminum fluoride structure may represent changes occurring during hydrolysis, because this structure is thought to mimic the transition state of hydrolysis (Fisher *et al.*, 1995). This closure could be inhibited by creation of mutations (e.g., E459V, C470G, N475K—corresponding to chicken residues E468, C479, N484 in Figure 1) in the region that may interact with complementary residues on the upper border of the cleft or residues that otherwise alter the conformation of the loop and helix that form the apex and lower border of the cleft. Interestingly, one of the myosin mutations recovered after random in vivo mutagenesis in *Dictyostelium* followed by selection for mutants that are cold-sensitive for myosin function changes a glutamic acid residue (E467K—chicken residue E485 in Figure 1, bottom) that may interact with the positively charged side chain of a residue forming part of the upper border of the cleft (Patterson and Spudich, 1996). The ability to use genetic screens to find intragenic suppressors of this mutation may potentially lead to identification of upper border residues that interact with this glutamic acid. The uniformity of biochemical defect despite a relatively broad spacing of these mutations supports the idea that conformational changes within this cleft region play an important role in hydrolysis of nucleotide and communication of this change at the active site to other regions of the myosin head. Current efforts include creation of S1 forms of several of these ATP nonhydrolyzers to test affinity for ATP and to characterize this hydrolysis defect more closely.

The final phenotypic class recovered in the screen consisted of myosins whose expression (at wild-type levels) only partially rescued the defects of the myosin null cells. Purification of several of these myosins revealed that they had biochemical defects that were variable but tended to be intermediate between those exhibited by the wild-type–like class myosins and the null class myosins. These intermediate class myosins shared the overall biochemical feature that their in vitro velocities were disproportionally lower than their solution ATPase activities, suggesting that, in some way, these mutations had resulted in partial uncoupling of ATPase and movement. Perhaps the most interesting of these uncouplers was the S465V (chicken residue S474 in Figure 1, bottom) myosin, which had an elevated basal ATPase activity in the absence of actin and exhibited only ~twofold activation of activity upon addition to actin. (Wild-type ATPase activity is typically activated > 10-fold by the addition of actin.) Despite an elevated ATPase activity, this myosin translocated actin filaments at only one-tenth the velocity of wild-type myosin. Placement of this residue on the structure reveals that it sits at the end of the long, lower border helix near the actin-binding face of the molecule. One intriguing possibility is that this change alters the conformation of this region of the cleft in such a way as to alter the communication between the ATP- and actin-binding sites so that the ATP-binding site "sees" a more actin-bound configuration even in the absence of actin; as a result, product release rates, which are affected by actin binding, would be "activated" relative to wild type. This would account for the elevated basal ATPase rate of this mutant and the relatively low extent of actin activation. The inefficient coupling of product release to actin rebinding in the prestroke state may account for the low sliding velocity of this myosin in vitro and its inability to completely rescue the defects of the myosin null cell in vivo. An alternative explanation for the behavior is that this mutation somehow affects the interaction of myosin with actin such that it increases the affinity for actin in either the weakly or strongly bound state. This would also account for the elevated actin-activated ATPase activity and the slower velocity in vitro. However, it would not account for the higher basal ATPase activity. Furthermore, mixing experiments in which this myosin

was placed on a surface with wild-type myosin gave rise to wild-type velocities of actin filaments, making it unlikely that these effects were due to increased affinity for actin.

The in vitro behaviors of the other members of the intermediate class are somewhat more difficult to interpret. They also exhibit very low sliding velocities relative to their solution ATPase activities. For example, the E476Q (chicken residue E485 in Figure 1, bottom) change has an actin-activated ATPase activity that is approximately the same as that of one of the wild-type–like class mutants (Y473S). However, the Y473S mutant moves actin filaments at > 10 times the velocity of the E476Q myosin. Unlike the S465V myosin, the other myosins in this class do not exhibit an elevation of their basal ATPase activities. Further characterization of these mutations, including a full kinetic analysis, is needed to better understand the nature of these biochemical defects. It is interesting to note that three of the four mutations that fall into this class are located on the side of the lower cleft helix that faces toward the actin-binding face of the molecule (yellow spheres in Figure 1, bottom stereo pair).

Overall, mutagenic analysis of this highly conserved region of the myosin motor domain supports the hypothesis derived from structural studies that this cleft plays a central role in the actomyosin–ATPase cycle. The behavior of the S465V (chicken residue S474 in Figure 1, bottom) myosin is consistent with the idea that this cleft participates in communication between the ATP and actin-binding sites. The defect in ATP hydrolysis exhibited by several of the more severe mutations suggests that this cleft must be able to alter its conformation for hydrolysis to take place. Further analysis of these mutated myosins as well as mutagenesis of other residues that line this cleft will lead to greater insights into the roles of this region in chemomechanical transduction. More generally, this study has shown the benefits of the combined in vivo and in vitro analysis of mutated myosins that are possible with the use of *Dictyostelium* and the added power of this approach when combined with the ability to analyze mutations in the context of high-resolution structural information.

ACKNOWLEDGMENTS

We thank Taro Uyeda and Bruce Patterson for helpful discussions and Dan Chasman for help with Figure 1. This work was supported by Grant GM-33289 to J.A.S. from the National Institutes of Health.

REFERENCES

Botts, J., Thomason, J.F., and Morales, M.F. (1989). On the origin and transmission of force in actomyosin. Proc. Natl. Acad. Sci. USA *86*, 2204–2208.

Bradford, M.M. (1976). A rapid and sensitive method for the quantitation of microgram quantities of protein utilizing the principle of protein–dye binding. Anal. Biochem. *72*, 248–254.

Clarke, M., and Spudich, J.A. (1974). Biochemical and structural studies of the actomyosin-like proteins from nonmuscle cells. Isolation and characterization of myosin from amoebae of *Dictyostelium discoideum*. J. Mol. Biol. *86*, 209–222.

Dayhoff, M.O. (1978). Atlas of Protein Sequence and Structure, Washington, DC: National Biomedical Research Foundation.

De Lozanne, A., and Spudich, J.A. (1987). Disruption of the *Dictyostelium* myosin heavy chain gene by homologous recombination. Science, *236*, 1086–1091.

Egelhoff, T.T., Lee, R.J., and Spudich, J.A. (1993). *Dictyostelium* myosin heavy chain phosphorylation sites regulate myosin filament assembly and localization in vivo. Cell *75*, 363–371.

Egelhoff, T.T., Manstein, D.J., and Spudich, J.A. (1990). Complementation of myosin null mutants in *Dictyostelium discoideum* by direct functional selection. Dev. Biol. *137*, 359–367.

Egelhoff, T.T., Titus, M.A., Manstein, D.J., Ruppel, K.M., and Spudich, J.A. (1991). Molecular genetic tools for study of the cytoskeleton in *Dictyostelium*. Methods Enzymol. *196*, 319–334.

Fisher, A.J., Smith, C.A., Thoden, J., Smith, R., Sutoh, K., Holden, H.M., and Rayment, I. (1995). Structural studies of myosin/nucleotide complexes: a revised model for the molecular basis of contraction. Biophys. J. *68*, 195–285.

Griffith, L.M., Downs, S.M., and Spudich, J.A. (1987). Myosin light chain kinase and myosin light chain phosphatase: effects of reversible phosphorylation on myosin structure and function. J. Cell Biol. *104*, 1309–1323.

Holmes, K.C., Popp, D., Gebhard, W., and Kabsch, W. (1990). Atomic model of the actin filament. Nature *347*, 44–49.

Huxley, H.E. (1969). The mechanism of muscular contraction. Science *164*, 1356–1366.

Huxley, H.E., and Kress, M. (1985). Cross-bridge behavior during muscle contraction. J. Muscle Res. Cell Motil. *6*, 153–161.

Itakura, S., Yamakawa, H., Toyoshima, Y.Y., Ishijima, A., Kojima, T., Harada, Y., Yanagida, T., Wakabayashi, T., and Sutoh, K. (1993). Force-generating domain of myosin motor. Biochem. Biophys. Res. Commun. *196*, 1504–1510.

Jontes, J.D., Kubalek, E.M.W., and Milligan, R.A. (1995). A 32° tail swing in brush border myosin I on ADP release. Nature *378*, 751–753.

Kabsch, W., Mannherz, H.G., Suck, D., Pai, E.F., and Holmes, K.C. (1990). Atomic structure of the actin/DNase I complex. Nature *347*, 37–44.

Kishino, A., and Yanagida, T. (1988). Force measurements by micromanipulation of a single-actin filament by glass needles. Nature *334*, 74–76.

Knecht, D.A., and Loomis, W.F. (1987). Antisense RNA inactivation of myosin heavy chain gene expression in *Dictyostelium discoideum*. Science *236*, 1081–1086.

Kraulis, P.J. (1991). MOLSCRIPT: A program to produce both detailed and schematic plots of protein structures. J. Appl. Crystallogr. *24*, 946–950.

Kronert, W.A., O'Donnell, P.T., and Bernstein, S.I. (1994). A charge change in an evolutionarily conserved region of the myosin globular head prevents myosin and thick filament accumulation in *Drosophila*. J. Mol. Biol. *236*, 697–702.

Kubalek, E.W., Uyeda, T.Q.P., and Spudich, J.A. (1992). A *Dictyostelium* myosin II lacking a proximal 58-kDa portion of the tail is functional in vivo and in vitro. Mol. Biol. Cell *3*, 1455–1462.

Kunkel, T.A., Roberts, J.D., and Zakour, R.A. (1987). Rapid and efficient site-specific mutagenesis without phenotypic selection. Methods Enzymol. *154*, 367–382.

Lowey, S., Waller, G.S., and Trybus, K.M. (1993). Skeletal muscle myosin light chains are essential for physiological speeds of shortening. Nature *365*, 454–456.

Lymn, R.W., and Taylor, E.W. (1971). Mechanism of adenosine triphosphate hydrolysis by actomyosin. Biochemistry *10*, 4617–4624.

Manstein, D.J., Titus, M.A., De Lozanne, A., and Spudich, J.A. (1989). Gene replacement in *Dictyostelium*: generation of myosin null mutants. EMBO J. *8*, 923–932.

Margossian, S.S., and Lowey, S. (1982). Preparation of myosin and its subfragments from rabbit skeletal muscle. Methods Enzymol. *85*, 55–71.

Maruta, H., and Korn, E.D. (1981). Direct photoaffinity labeling by nucleotides of the apparent catalytic site on the heavy chains of smooth muscle and *Acanthamoeba* myosins. J. Biol. Chem. *256*, 499–502.

Patterson, B., and Spudich, J.A. (1996). Cold-sensitive mutations of *Dictyostelium* myosin heavy chain highlight functional domains of the myosin motor. Genetics *143*, 801–810.

Peltz, G., Spudich, J.A., and Parham, P. (1985). Monoclonal antibodies against seven sites on the head and tail of *Dictyostelium* myosin. J. Cell Biol. *100*, 1016–1023.

Perrie, W.T., Smillie, L.B., and Perry, S.V. (1973). A phosphorylated light chain component of myosin from skeletal muscle. Biochem. J. *135*, 151–164.

Rayment, I., Holden, H.M., Whittaker, M., Yohn, C.B., Lorenz, M., Holmes, K.C., and Milligan, R.A. (1993a). Structure of the actin–myosin complex and its implications for muscle contraction. Science *261*, 58–65.

Rayment, I., Rypniewski, W., Schmidt-Base, K., Smith, R., Tomchick, D., Benning, M.M., Winkelmann, D.A., Wesenberg, G., and Holden, H.M. (1993b). The three-dimensional structure of myosin subfragment-1: a molecular motor. Science *261*, 50–58.

Reedy, M.K. (1993). Myosin–actin motors: the partnership goes atomic. Structure *1*, 1–5.

Ruppel, K.M., Uyeda, T.Q.P., and Spudich, J.A. (1994). Role of highly conserved lysine 130 of myosin motor domain: in vivo and in vitro characterization of a site specifically mutated myosin. J. Biol. Chem. *269*, 18773–18780.

Sambrook, J., Fritsch, E.F., and Maniatis, T. (1989). Molecular Cloning: A Laboratory Manual, 2nd ed., Cold Spring Harbor, NY: Cold Spring Harbor Laboratory Press.

Schroeder, R.R., Manstein, D.J., Jahn, W., Holden, H., Rayment, I., Holmes, K.C., and Spudich, J.A. (1993). Three-dimensional atomic model of F-actin decorated with *Dictyostelium* myosin S1. Nature *364*, 171–174.

Sellers, J.R., and Goodson, H.V. (1995). Motor proteins 2: myosin. Protein Profile *1*, 1323–1423.

Spudich, J.A. (1989). In pursuit of myosin function. Cell Regul. *1*, 1–11.

Spudich, J.A., Finer, J., Simmons, B., Ruppel, K., Patterson, B., and Uyeda, T. (1995). Myosin structure and function. Cold Spring Harbor Symp. Quant. Biol. 60, 783–791.

Spudich, J.A., and Watt, S. (1971). The regulation of rabbit skeletal muscle contraction. I. Biochemical studies of the interaction of the tropomyosin–troponin complex with actin and the proteolytic fragments of myosin. J. Biol. Chem. *246*, 4866–4871.

Sutoh, K., Tokunaga, M., and Wakabayashi, T. (1989). Electron microscopic mappings of the myosin head with site-directed antibodies. J. Mol. Biol. *206*, 357–363.

Toyoshima, Y.Y., Kron, S.J., McNally, E.M., Niebling, K.R., Toyoshima, C., and Spudich, J.A. (1987). Myosin subfragment-1 is sufficient to move actin filaments in vitro. Nature *328*, 536–539.

Uyeda, T.Q.P., Abramson, P.D., and Spudich, J.A. (1996). The neck region of the myosin motor domain acts as a lever arm to generate movement. Proc. Natl. Acad. Sci. USA *93*, 4459–4464.

Uyeda, T.Q.P., Kron, S.J., and Spudich, J.A. (1990). Myosin step size: estimation from slow sliding movement of actin over low densities of heavy meromyosin. J. Mol. Biol. *214*, 699–710.

Uyeda, T.Q.P., Ruppel, K.M., and Spudich, J.A. (1994). Enzymatic activities correlate with chimaeric substitutions at the actin-binding face of myosin. Nature *368*, 567–569.

Uyeda, T.Q.P., and Spudich, J.A. (1993). A functional recombinant myosin II lacking a regulatory light chain-binding site. Science *262*, 1867–1870.

Warshaw, H.M., Derosiers, J.M., Work, S.S., and Trybus, K.M. (1990). Smooth muscle myosin cross-bridge interactions modulate actin filament sliding velocity in vitro. J. Cell Biol. *111*, 453–463.

Whittaker, M., Kubalek, E.M.W., Smith, J.E., Faust, L., Milligan, R.A., and Sweeney, H.L. (1995). A 35-Å movement of smooth muscle myosin on ADP release. Nature *378*, 748–751.

Yanisch-Perron, C., Vieira, J., and Messing, J. (1985). Improved M13 phage-cloning vectors and host strains: nucleotide sequences of the M13mp18 and pUC19 vectors. Gene *33*, 103–119.